2017 IEEE International Conference on Robotics and Automation (ICRA)
Singapore, May 29 - June 3, 2017

Velocity characterization and control strategies for nano-robotic systems based on piezoelectric stick-slip actuators

Shuai Liang[1], Mokrane Boudaoud[1], Barthélemy Cagneau[2] and Stéphane Régnier[1]

***Abstract*— Nano-robotic systems based on Piezoelectric Stick-Slip (PSS) actuators have become increasingly popular in research and industry for semi-automated and automated tasks at small scales. For an efficient use of PSS actuators, a series of research have been fulfilled on design process, dynamic modeling, driving methods and position control. However, there have been very few investigations on velocity control of PSS actuators. Velocity control is important to enable the nano-robotic system to generate a smooth and efficient motion and to avoid the undesired inertial shock of the end effector. This paper deals with velocity characterization and control strategies for nano-robotic systems based on PSS actuators. The range of achievable velocities on PSS actuators is studied in air and vacuum environments. This analysis allows the definition of a detailed map of the velocity characteristics in forward and backward directions of motion. Velocity control strategies are then studied based on an instantaneous velocity feedback and an average velocity feedback. Results of the proposed method show the first experimental demonstration of velocity control for PSS actuators in medium and high speed configurations opening new perspectives on the use of nano-robotic systems in dynamic automated tasks.**

I. INTRODUCTION

NOWADAYS, nano-robotic systems are a compelling solution for laboratories and industries to deal with automated robotic tasks at the micrometer and the nanometer scales [1]. This is due to their high positioning resolution and precision which enable researchers and engineers to meet the harsh requests of the physics at the small scales. Nanorobotic systems are a key technology widely used in various applications, such as nanomanipulation [2][3], nanoassembly [4][5], electrical characterization [6][7][8], and mechanical characterization [9] of nano-materials.

The Piezoelectric Stick-Slip (PSS) [10] [11] [12] is one of the most used actuator in nano-robotic systems because of its ability to produce a coarse displacement in the millimeter or the micrometer ranges and a fine displacement with a nanometer resolution. It has also several advantages compared to other classes of actuators in terms of cost, control design and miniaturization potential.

Various research have been conducted on PSS actuators to constantly go further towards better performances. In [12], a novel analog electronic driver for PSS actuators has been designed. It features a charge control to reduce the effect of the hysteresis and a switching scheme to achieve a high slew rate with an admissible heat dissipation. In [13], a mechanism has been designed to satisfy performance robustness against the load variations on the actuator. New driving methods for piezoelectric inertia drives have been studied in [14]. In a recent work [15], an augmented elasto-plastic friction model has been proposed to simulate the dynamic motion of such actuators in backward and forward motion directions. A comprehensive research on design, position control, and performance analysis of a PSS actuator has been presented in [16]. In [17], a 2-dof stick-slip system has been developed, modeled and controlled. The authors have proposed in [18] a voltage/frequency proportional method to control the position of this system. In addition, several compagnies such as SmarAct, Physik Instrumente and Attocube, are focussing on the design of novel PSS actuators for high precision mechanical industry.

According to the current state of the art, there are a series of research related to mechanical design, sensor technology, friction materials, non-linear dynamic modeling and position control methods. However, there has been very few research on the velocity control of a stick-slip system until now. Velocity control is fundamental in many robotic applications. Without such a control structure, the nano-robotic system may generate undesired inertial shock of the end effector during the conversions between different motion phases [19]. Especially, at micrometer and nanometer scales, these vibrations may be large enough to cause the destruction of a nano-material or to shake off the object to be manipulated. A robust and efficient velocity control enable the nano-robotic system to generate a smooth motion along a desired trajectory without excessive vibrations.

In this paper, we propose a comprehensive study on velocity characterization and control for nano-robotic systems based on PSS actuators. The work fills the technological gap in nano-robotics for applications requiring a motion generation at the micrometer and the nanometer scales with a controlled speed. In order to provide velocity references that PSS actuators can achieve, experiments are carried in both forward and backward directions of motion under air and vacuum environments. Through applying various input sawtooth voltages on the actuator with different amplitudes and frequencies, the velocity range of the actuator is identified. This analysis allows obtaining a detailed map of the velocity characteristics in forward and backward directions of motion. Velocity control strategies are then studied and implemented experimentally on a nano-robotic system. The control method

[1]Shuai Liang, Mokrane Boudaoud and Stéphane Régnier are with the Sorbonne Universités, UPMC University Paris 06, UMR 7222, ISIR, F-75005 Paris, France.- liang@isir.upmc.fr, mokrane.boudaoud@isir.upmc.fr, stephane.regnier@upmc.fr.

[2]Barthélemy Cagneau is with the Université de Versailles St-Quentin en Yvelines / LISV, 10-12 Avenue de l'Europe, 78140, France. barthelemy.cagneau@uvsq.fr

978-1-5090-4633-1/17/$31.00 ©2017 IEEE

is based on a Proportional Integral (PI) scheme to control the amplitude and the frequency of a sawtooth input voltage. Two control strategies are studied, the first one uses the instantaneous velocity of the actuator as a feedback signal and the second one uses, at each sampling time, the slope value of the displacement from the actuator's starting position as the closed loop feedback. The performance of each strategy in terms of stability and tracking capabilities is evaluated with both simulation and experimental data. The achieved controlled velocities are ranging from 500 μm/s to 5000 μm/s. Results of the proposed methods open new perspectives for the dynamic control of nano-robotic systems.

The paper is organized as follows. In section II, the experimental setup including the studied nano-robotic system and the control unit is described. Section III deals with the non-linear model of an elementary PSS actuator as proposed in [15]. The velocity characterization of the actuator in air and vacuum environments is presented in section IV. The velocity control strategies and the experimental results are presented in section V. Sections VI concludes the paper.

II. Experimental Setup

The experimental setup is composed of (see Fig. 1): (i) a multi-dof nano-robotic system based on PSS actuators [20], (ii) digital interpolators, (iii) a real time controller board (dSPACE DS1007), (iv) a control desk monitor (dSPACE ControlDesk), (v) a Scanning Electron Microscope (ZEISS EVO), and (vi) a high frequency sawtooth signal generator.

The nano-robotic system has 9 PSS actuators assembled in such a way to construct a multi-dof kinematic structure. It is composed of a 3 dof serial structure and a 6 dof parallel structure (Fig. 1.b). All the actuators are from the same series (SLC-1720-S-HV). The digital interpolators are connected to the encoder position sensor of each actuator to obtain a measurement resolution of 5 nm. The real time controller board is used for the implementation of the closed loop control algorithms. The control desk monitor allows the human operator to communicate in real time with the nano-robotic system (e.g. changing in real time the control parameters, the reference position, the reference velocity, etc.). The sawtooth generator has been designed with a digital signal processor. This generator allows modifying the amplitude, the frequency and the direction of the output signal in real time. The amplitude range and the frequency range of the generated sawtooth voltage are [50 Hz- 11 kHz] and [0 V- 5 V] respectively. The sawtooth voltage is amplified by a factor of 20 to drive the piezoelectric element of a PSS actuator.

III. Dynamic non-linear model of the nano-robotic system

The elementary structure of a PSS actuator includes a Piezoelectric Element (PE), a slider and a friction material as shown in Fig. 2.a. Each axis of the nano-robotic system is attached to the slider of an actuator. The slider sticks to the PE when the latter has a slow deformation. The stick phase occurs during the slow positive or negative slope of

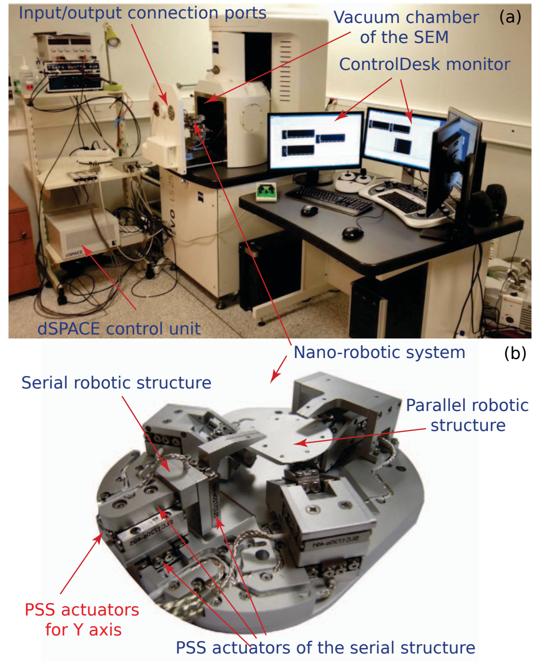

Fig. 1. (a) Experimental control setup for the nano-robotic system inside a Scanning Electron Microscope (SEM). (b) Enlarged view of the multi-dof nano-robotic system based on PSS actuators.

the sawtooth voltage. The slider slips along the PE when the latter is abruptly deformed. The slip phase occurs during the rising or the falling edges of the sawtooth voltage.

When the slider follows the motion of the PE, the actuator is working in *scanning mode*. In the case of several sequences of stick and slip motions of the slider, the actuator is working in *stepping mode*. In this case, the motion direction of the slider, i.e. forward or backward, is governed by the sign of ramp slope of the sawtooth input voltage.

In a recent work [21], we have proposed a new non-linear dynamic model of a PSS actuator. The model is based on an augmented voltage/frequency modeling of the friction force considering a multi-state elasto-plastic formulation.

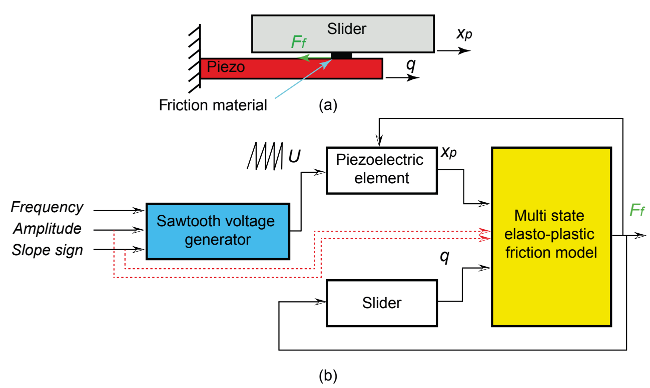

Fig. 2. (a) Simplified scheme of a PSS actuator. (b) Block diagram of the non-linear model of a PSS actuator proposed in [21]. x_p and q are respectively the motion of the PE and that of the slider, F_f is the friction force and U is the input voltage. The input and the output of the model are U and q respectively.

The model takes into account the dynamics of the PE, of the slider and that of the friction force F_f. The block diagram of the non-linear model is shown in Fig. 2.b. This model will be used to define the gains of the controller in section V.

IV. Analysis and Characterization of the Velocity

Because nano-robotic systems are not only used in air environment but also in the vacuum chamber of a Scanning Electron Microscope (SEM) for some specific applications [22][3][4][5][6], the velocity characterization is done in both air and vacuum. Without loss of generality, all experiments are performed on the PSS actuator of Y axis in the serial nano-robotic structure (see Fig. 1.b).

The aim is to define the reachable velocities of the actuator based on the experimental conditions. Experiments have shown that the velocity of the slider depends mainly on the sawtooth voltage parameters, namely the amplitude, the frequency and the sign of the ramp slope.

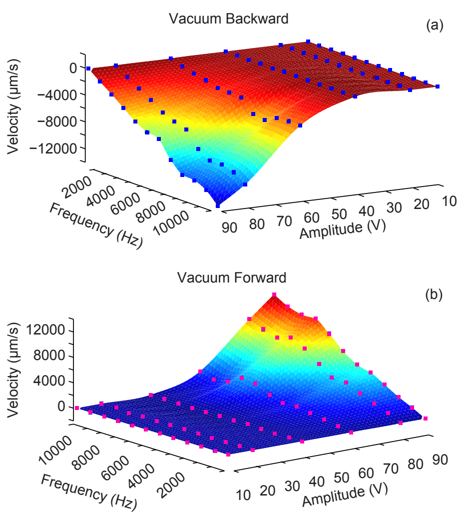

Fig. 3. Velocity characteristics of the piezoelectric stick-slip actuator in vacuum environment.

The experiments have been done first in air and then in vacuum under the following protocol: (i) a sawtooth voltage with a fixed amplitude, frequency and ramp slope is applied on the piezoelectric element of the actuator, (ii) the displacement of the slider is measured during several seconds with 35 kHz sampling frequency using the integrated optical encoder, (iii) the average velocity is calculated based on the experimental displacement measurement. This experiment is repeated for sawtooth voltages with the following frequencies: 50 Hz, 1 kHz, 2 kHz, 3 kHz, 4 kHz, 5 kHz, 6 kHz, 7 kHz, 8 kHz, 9 kHz, 10 kHz and 11 kHz. For each frequency, different amplitudes are applied, namely 10 V, 20 V, 40 V, 60 V, 80 V and 90 V. The same experiment is then repeated by changing the sign of the ramp slope of the sawtooth voltage. In total, the average velocity of the actuator has been identified for 144 operating points in air and 144 operating points in vacuum. In this latter case, the

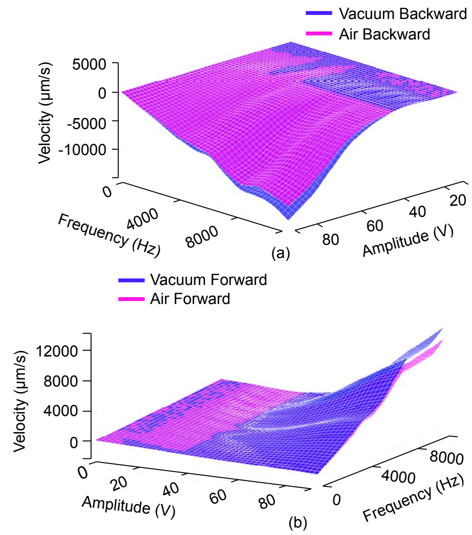

Fig. 4. Velocity characteristics of the PSS actuator in air and vacuum environments for backward (a) and forward (b) motion directions.

nano-robotic system has been put inside the SEM with a vacuum pressure of 3.16×10^{-4} Pa.

For each operating condition, i.e. air/forward direction, vacuum/forward direction, air/backward direction and vacuum/backward direction, the velocity characteristic of the actuator with respect to the amplitude and the frequency of the sawtooth voltage has been obtained. Fig. 3 shows the result of this characterization in vacuum environment. The curve has been obtained by fitting the experimentally identified average velocities using a cubic interpolation.

These curves provide several information for the analysis of the velocity in PSS actuators. For a given set of amplitude and frequency, the slider moves faster in backward direction. This is observed in both air and vacuum conditions. The velocity does not depend on the sawtooth voltage parameters only, but also on the working environment. Indeed, with the same input amplitude, input frequency and motion direction, the actuator moves faster in vacuum than in air as shown in Fig. 4. The difference of velocity in air and vacuum is significant only for velocities higher than 10000 μm/s. The minimum and the maximum identified velocities for each operating condition are summarized in Table I.

For control purposes, the velocity characteristic curves allow the definition of the required amplitude and the re-

	Air		Vacuum	
	Forward	Backward	Forward	Backward
Maximum Velocity [μm/s]	10732	-11465	12313	-13796
Minimum Velocity [μm/s]	17	-30.9203	21.9235	-37.473

TABLE I

Maximum and minimum measured velocities in different operating conditions.

quired frequency of the sawtooth voltage to reach a desired velocity. It can also be used as a basis for the definition of the proportional gains to control the amplitude and the frequency of the sawtooth voltage in closed loop so that the actuator can reach a reference velocity.

V. Velocity control strategies

Velocity control strategies are proposed in this section considering the range [500 μm/s - 5000 μm/s]. As shown in Fig. 4, the effect of the environment (i.e. air and vacuum) on the velocity in this range is not very high. As such, velocity control in both environments using the same controller will lead to comparable results. Therefore, in this section experiments are performed in vacuum only.

The first strategy is based on the instantaneous velocity while the second one uses the average velocity calculated at each sampling time from the actuator's starting position.

A. *Instantaneous velocity control*

The velocity control is based on two Proportional-Integral (PI) controllers. As shown in Fig. 5, PI controller 1 and PI controller 2 are used to control the amplitude and the frequency respectively of the driving sawtooth voltage. The input of each controller is the error between the reference velocity V_{ref} and the actual instantaneous velocity v_i. The output of the *sign* function allows the definition of the direction of motion of the actuator.

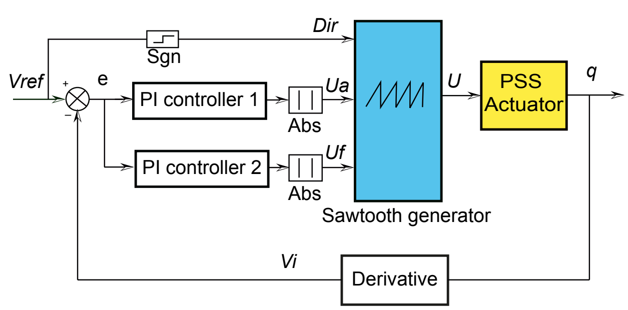

Fig. 5. Control diagram of the closed loop instantaneous velocity control. V_{ref} and V_i are respectively the desired velocity reference and the actual instantaneous velocity of the slider.

The controller is designed in the discrete form as follows:

$$U_a(k) = K_{pa}e(k) + \sum_{i=1}^{k}(K_{ia}e(k)T_e) \qquad (1)$$

$$U_f(k) = K_{pf}e(k) + \sum_{i=1}^{k}(K_{if}e(k)T_e) \qquad (2)$$

The signals $U_a(k)$ and $U_f(k)$ are calculated from the PI controllers. They define respectively the amplitude and the frequency of the sawtooth voltage. K_{pa}, K_{ia} are the proportional gain and the integral gain respectively of PI controller 1. K_{pf}, K_{if} are the proportional gain and the integral gain respectively of PI controller 2. T_e is the sampling time and kT_e stands for the time. The derivative of the displacement is considered as the feedback signal.

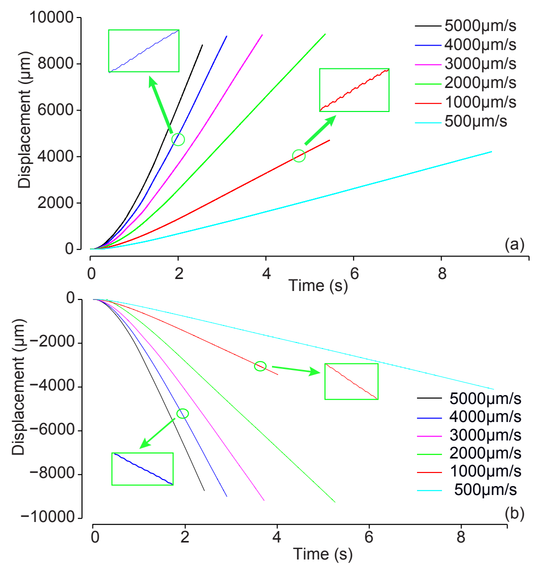

Fig. 6. Experimental results of the displacement of the slider with the closed loop instantaneous velocity control. (a) Displacement in forward direction. (b) Displacement in backward direction. The PSS actuator is operating in the vacuum environment.

Since the actuator is driven by a stick-slip principle, the instantaneous velocity used in the feedback loop becomes very high during the slip phases. This is a major impediment to achieve a good compromise between the closed loop bandwidth and the stability margin of the system. For instance, high gains of the controller lead to a fast response time but significant vibrations of the actuator will be produced.

For the implementation of the controller, based on a trade off between stability and response time, the selected gains are $K_{pa} = 0.00001\ Vs/\mu m$, $K_{ia} = 1.2\ Vs/\mu m$, $K_{pf} = 0.001\ Vs/\mu m$ and $K_{if} = 1\ Vs/\mu m$.

The controller has been designed using matlab/simulink and the implementation has been performed on the dSPACE controller board with a sampling frequency of 35 kHz. The control voltages U_a and U_f calculated with the controller board are connected to the input of the sawtooth generator to drive the PSS actuator.

The velocity references have been selected taking into account the characterization results of Fig. 3. Experimental results of the slider displacement with the closed loop instan-

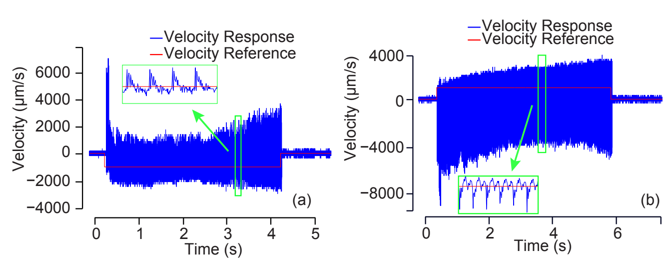

Fig. 7. Experimental instantaneous velocity of the slider with the closed loop feedback for a reference of 1000 μm/s. (a) Velocity in forward direction. (b) Velocity in backward direction. The PSS actuator is operating in the vacuum environment.

taneous velocity control are shown in Fig. 6 for reference velocities of 500 μm/s, 1000 μm/s, 2000 μm/s, 3000 μm/s, 4000 μm/s and 5000 μm/s. For the evaluation of the controller performance, experiments have been performed in forward and backward directions.

For PSS actuators, using an instantaneous velocity control leads to a relatively long response time which is more than 1 s in the range of the input reference [500 μm/s - 5000 μm/s]. This is an important issue for PSS actuators, which have a limited working range. For instance, the displacement range of the studied actuator is 12 mm. Using a reference velocity of 5000 μm/s, the actuator reaches the desired velocity in closed loop after having traveled the half of the total displacement range. Moreover, there are significant vibrations in the instantaneous velocity feedback signal as shown in Fig. 7. This is mainly due to the repetition of several sequences of slip motions.

The instantaneous velocity control is an interesting solution for PSS actuators but it requires a severe compromise between stability and response time.

B. Average velocity control

The velocity of the slider can also be calculated by the ratio between the displacement and the time, i.e. the slope of the displacement with respect to the time. The velocity control describes the instant velocity state, and the slope control reflects the average velocity state. If a velocity control is applied, the average velocity must also converge to the velocity reference.

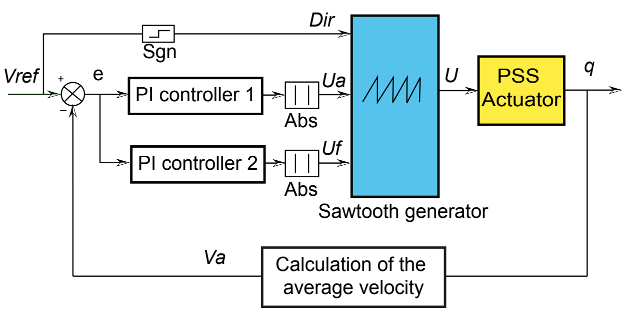

Fig. 8. Control diagram of the closed loop average velocity control. V_{ref} and V_a are respectively the desired velocity reference and the actual average velocity calculated from the slider's starting position.

The average velocity is calculated by

$$V_a = \frac{q}{t - t_0} \tag{3}$$

Where V_a is the average velocity, q represents the displacement of the slider, t stands for the actual time and t_0 is the time when the slider starts moving (initial position).

The control diagram is shown in Fig. 8. It has the same working principle as that of the previous controller (Fig. 5) except that the output feedback is now the average velocity.

The ratio between the total displacement of the slider and the unwanted vibration generated at the slip phase is high. Therefore, the effect of the slip vibrations on the velocity

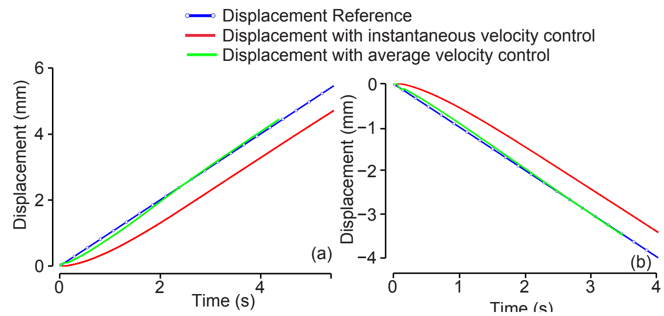

Fig. 9. Experimental results of the displacement of the slider with the closed loop average velocity control and instantaneous velocity control for a velocity reference of 1000 μm/s. (a) Displacement in forward direction. (b) Displacement in backward direction. The PSS actuator is operating in the vacuum environment.

control performance is very limited. With the average velocity control, it is then possible to find a good tradeoff between the stability and the response time. The gains of the controller can be increased to decrease the closed loop response time while keeping a safe stability margin.

For the implementation of the controller, the selected gains are $K_{pa} = 1\ Vs/\mu$m, $K_{ia} = 0.8\ Vs/\mu$m, $K_{pf} = 1.2\ Vs/\mu$m and $K_{if} = 2.5\ Vs/\mu$m.

The controller has been implemented in the controller board. Experimental results of the displacement of the slider with the closed loop average velocity control and the instantaneous velocity control for a velocity reference of 1000 μm/s are shown in Fig. 9. This result demonstrates the ability to converge faster to a target position with a controlled average velocity. Thus, the slider's displacement curve is able to track and converge to the integral curve of the constant velocity reference.

Closed loop position tracking of a triangle wave when using the average velocity control and the instantaneous velocity control are shown in Fig. 10 and Fig. 11 respectively. The input reference is a square velocity signal of 0.2 Hz with -500 μm/s and +500 μm/s minimum and maximum values respectively. For tracking performance, the advantage of using the average velocity feedback to control the velocity of PSS actuators is demonstrated. The results have been compared with simulation data using the model presented in section III. For the simulation, the controller gains have been selected equal to those used in the experiments. A good agreement is observed between simulation and experimental data. This result opens new perspectives on the use of a dynamic model of PSS actuators for the definition of closed loop control parameters.

VI. Conclusion

Nano-robotic systems using Piezoelectric Stick-Slip actuators (PSS) are a key solution in research and industry for automated tasks at small scales. This paper has dealt with the issue of velocity characterization and control in PSS actuators. An analysis and a characterization of the achievable velocities for this class of actuators have been

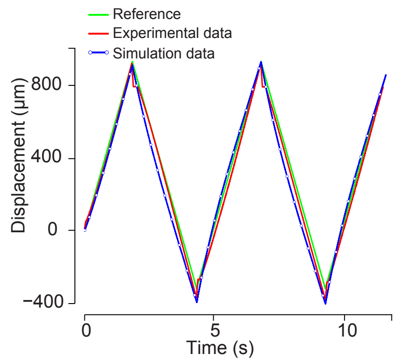

Fig. 10. Simulation and experimental tracking results with the closed loop average velocity control. The reference velocity is ±500 μm/s. The PSS actuator is operating in the vacuum environment.

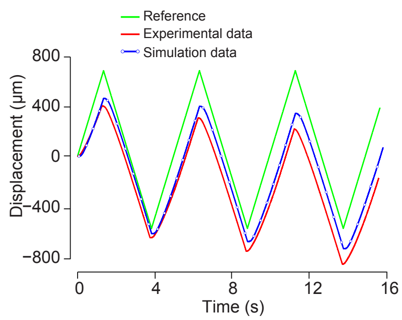

Fig. 11. Simulation and experimental tracking results with the closed loop instantaneous velocity control. The reference velocity is ±500 μm/s. The PSS actuator is operating in the vacuum environment.

conducted. For a fixed amplitude and a fixed frequency of the input sawtooth voltage, it has been demonstrated that the velocity is mainly affected by two parameters, the motion direction and the working environment (air and vacuum). The velocity characteristic curve has been used as a basis for the definition of the range of input velocity references that can be used for the control. Velocity control strategies have then been studied based on an instantaneous velocity feedback and an average velocity feedback. The performance analysis of each strategy in terms of stability and tracking capabilities has been studied and highlighted. For the best knowledge of the authors, this paper has presented the first comprehensive study on the characterization and the velocity control for PSS actuators in medium speed and high speed configurations and in both air and vacuum conditions. Future works will deal with the control of multi-dof nano-robotic systems using haptic interfaces with a velocity tracking capability.

References

[1] N. Chaillet and S. Régnier, *Microrobotics for Micromanipulation*. John Wiley Sons, Inc, 2010.

[2] M. Boudaoud, Y. L. Gorrec, Y. Haddab, and P. Lutz, "Gain scheduling control of a nonlinear electrostatic microgripper: Design by an eigenstructure assignment with an observer-based structure," *IEEE Transactions on Control Systems Technology*, vol. 23, no. 4, pp. 1255–1267, July 2015.

[3] S. Qin, T.-H. Kim, Z. Wang, and A.-P. Li, "Nanomanipulation and nanofabrication with multi-probe scanning tunneling microscope: From individual atoms to nanowires," *Review of Scientific Instruments*, vol. 83, no. 6, 2012. [Online]. Available: http://scitation.aip.org/content/aip/journal/rsi/83/6/10.1063/1.4727878

[4] V. Eichhorn, M. Bartenwerfer, and S. Fatikow, "Nanorobotic assembly and focused ion beam processing of nanotube-enhanced afm probes," *IEEE Transactions on Automation Science and Engineering*, vol. 9, no. 4, pp. 679–686, 2012.

[5] Z. Yang, M. Nakajima, Y. Shen, and T. Fukuda, "Assembly and evaluation of mwcnts probe thermal sensor by nanorobotic manipulation," in *Nanotechnology (IEEE-NANO), 2012 12th IEEE Conference on*, Aug 2012, pp. 1–4.

[6] C. Ru, Y. Zhang, Y. Sun, Y. Zhong, X. Sun, D. Hoyle, and I. Cotton, "Automated four-point probe measurement of nanowires inside a scanning electron microscope," *IEEE Transactions on Nanotechnology*, vol. 10, no. 4, pp. 674–681, July 2011.

[7] Y. L. Zhang, Y. Zhang, C. Ru, B. Chen, and Y. Sun, "A load-lock-compatible nanomanipulation system for scanning electron microscope," *Mechatronics, IEEE/ASME Transactions on*, vol. 18, no. 1, pp. 230–237, Feb 2013.

[8] M. Elawayeb, Y. Peng, K. J. Briston, and B. J. Inkson, "Electrical properties of individual nife/pt multilayer nanowires measured in situ in a scanning electron microscope," *Journal of Applied Physics*, vol. 111, no. 3, pp. –, 2012.

[9] S. T. Boles, A. Sedlmayr, O. Kraft, and R. Monig, "In situ cycling and mechanical testing of silicon nanowire anodes for lithium-ion battery applications," *Applied Physics Letters*, vol. 100, no. 24, 2012.

[10] C. Belly and W. Charon, "Benefits of amplification in an inertial stepping motor," *Mechatronics*, vol. 22, no. 2, pp. 177–183, 2012.

[11] C.-F. Yang, S.-L. Jeng, and W.-H. Chieng, "Motion behavior of triangular waveform excitation input in an operating impact drive mechanism," *Sensors and Actuators A: Physical*, vol. 166, no. 1, pp. 66–77, 2011.

[12] M. Špiller and Z. Hurák, "Hybrid charge control for stick–slip piezoelectric actuators," *Mechatronics*, vol. 21, no. 1, pp. 100–108, 2011.

[13] Y. Wang, J. Zhu, M. Pang, J. Luo, S. Xie, M. Liu, L. Sun, C. Zhou, M. Tan, J. Ge, Y. Sun, and C. Ru, "A stick-slip positioning stage robust to load variations," *IEEE/ASME Transactions on Mechatronics*, vol. PP, no. 99, pp. 1–1, 2016.

[14] M. Hunstig, T. Hemsel, and W. Sextro, "Stick?slip and slip?slip operation of piezoelectric inertia drives. part i: Ideal excitation," *Sensors and Actuators A: Physical*, vol. 200, pp. 90 – 100, 2013.

[15] T. Lu, M. Boudaoud, D. Hériban, and S. Régnier., "Nonlinear modeling for a class of nano-robotic systems using piezoelectric stick-slip actuators," in *IEEE/RSJ International Conference on Intelligent Robots and Systems, Hamburg, Germany.*, 2015.

[16] J. M. Breguet and R. Clavel, "Stick and slip actuators: design, control, performances and applications," in *Micromechatronics and Human Science, 1998. MHS '98. Proceedings of the 1998 International Symposium on*, Nov 1998, pp. 89–95.

[17] M. Rakotondrabe, Y. Haddab, and P. Lutz, "Development, modeling, and control of a micro-/nanopositioning 2-dof stick-slip device," *Mechatronics, IEEE/ASME Transactions on*, vol. 14, no. 6, pp. 733–745, Dec 2009.

[18] M. Rakotondrabe, Y. Haddab, and P. Lutz, "Voltage/frequency proportional control of stick-slip micropositioning systems," *IEEE Transactions on Control Systems Technology*, vol. 16, no. 6, pp. 1316–1322, Nov 2008.

[19] W. Khalil and E. Dombre, *Modeling, Identification and Control of Robots*. Kogan Page Science Paper Edition, 2006.

[20] J.-O. Abrahamians, B. Sauvet, J. Polesel-Maris, R. Braive, and S. Régnier, "A nanorobotic system for in situ stiffness measurements on membranes," *IEEE Transactions on Robotics*, vol. 30, pp. 119–124, 2013.

[21] M. Boudaoud, T. Lu, S. Liang, R. Oubellil, and S. Régnier., "Voltage/frequency rate dependent modeling for nano-robotic systems based on piezoelectric stick-slip actuators," in *IEEE/RSJ International Conference on Intelligent Robots and Systems, Deajeon, South Korea*, 2016.

[22] M. Takahashi, H. Ko, T. Ushiki, and F. Iwata, "Interactive nano manipulator based on an atomic force microscope for scanning electron microscopy," in *International Symposium on Micro-NanoMechatronics and Human Science (MHS)*, 2011, pp. 495–500.